An Investigation of Signal Characteristics and T_1 Relaxation Time in Brain MR Images of Young versus Old Healthy Adults

Hayriye Aktaş Dinçer[1] and Didem Gökçay[2]

[1]*Department of Biomedical Engineering, Graduate School of Natural and Applied Sciences,*
Middle East Technical University, Dumlupinar Bulvari, 06800 Ankara, Turkey
[2]*Department of Health Informatics, Informatics Institute, Middle East Technical University,*
Dumlupinar Bulvari, 06800 Ankara, Turkey

Keywords: Brain Aging, Spin Lattice Relaxation Time (T_1), T_1 Mapping, Signal-to-Noise Ratio (SNR), Contrast to Noise Ratio (CNR), Gray-White Ratio (GWR), Segmentation.

Abstract: During healthy aging, the brain undergoes several structural changes such as atrophy and volumetric changes. Although less evident, changes in tissue concentration also occur. Such differences in brain tissues introduce prominent low contrast effects to the MRI images of the aging population, causing segmentation problems in the data processing pipeline. Measures of tissue characteristics such as T_1 provide unique and complementary information to widely used measures of brain signal characteristics. In this study, multiple Fast Low Angle Shot (FLASH) images are collected for T_1 mapping of whole brains from young and old adults. Tissue signal characteristics are evaluated on predefined regions and compared across Magnetization Prepared Rapid Gradient Echo (MPRAGE) and T_1 maps. Additionally, segmentation performance is analyzed. As a result, we found that T_1 maps are superior to MPRAGE protocol in terms of contrast, especially within sub-cortical areas. Furthermore, degradation of grey-white-ratio (GWR) due to aging processes is observed to be less pronounced in T_1 estimated whole brain images. Moreover, sensitivity of T_1 maps (54.6%) are higher than MPRAGE images (34.4%) in detection of sub-cortical gray matter. In sum we concur that T_1 maps provide better avenues to investigate age related morphological changes in the brain.

1 INTRODUCTION

Even in the absence of neurological disorder, aging brains show alterations (Resnick et al., 2000; Thambisetty et al., 2010). These age-dependent alterations affect the imaging properties of the brains (Salat et al., 2009). Revealing the alterations derived from healthy aging provides crucial foundation for understanding age related brain diseases (Tau and Bradley, 2010).

Morphological changes in aging brains like brain atrophy, reduction of grey matter (GM) and white matter (WM), ventricular enlargement and decrease of cortical thickness are well documented (Resnick et al., 2000; Courchesne et al., 2000; Salat et al., 2004; Ge et al., 2002). T_1 longitudinal relaxation time provides valuable information about underlying tissue microarchitecture. T_1 relaxation time is affected by myelin and iron concentrations in brain tissue. Increased demyelination elongates the T_1 value, while iron accumulation shortens it (Ogg and

Steen, 1998). Iron and manganese accumulation in deep GM and WM demyelination and axonal loss are common in aging brains. Hence these alterations can influence T_1 relaxation time of the underlying tissue and thereby imaging properties and contrast (Desmond et al., 2016). This is an important problem which distorts the diagnosis and segmentation procedures. The signal alterations derived from aging are less studied in literature. T_1 maps provide a more robust template for morphometry studies like segmentation and a more specific marker of disease progression in comparison to conventional T_1 weighted images.

The aim of this work is to investigate signal characteristics in young and old healthy brains using conventional MR protocols, to decide whether T_1 weighted images or estimated T_1 maps provide better image quality. 19 healthy volunteers were scanned with MPRAGE and FLASH sequences, and then T_1 relaxation time of whole brain was mapped via variable flip angle (VFA) method. In order to evaluate

the image quality contrast, gray-white-ratio (GWR), signal-to-noise ratio (SNR) and contrast-to-noise ratio (CNR) were calculated on 5 predefined specific Regions of Interest (ROI). Additionally, subcortical area of MPRAGE and T_1 maps were segmented. The performance of both images were presented as sensitivity and specificity measurements.

2 METHOD

First of all, whole brain was scanned with MPRAGE protocol. Then 4 brain images that adhered to the same imaging coordinates with the MPRAGE sequence were collected with FLASH sequence with varying flip angles.

Afterwards whole brain T_1 maps were constructed with the help of an in-house developed MATLAB script. To be able to identify and compare signal characteristics of MPRAGE and T_1 maps as well as differences across young and old adults signal to noise ratio (SNR), contrast to noise ratio (CNR) and grey white ratio (GWR) are calculated for specific landmarks.

Additionally, both MPRAGE and T_1 map images were brain extracted via FSL BET (Brain Extraction Tool) (Smith, 2002), then aligned to a standard stereotaxic space and subcortical area were segmented. Sensitivity and specificity of MPRAGE and T_1 maps were evaluated and also segmentation performance in both age group investigated.

2.1 Subject Profile

9 young (6 M, 3 F, age: 31.33±4.59) and 10 old (2 M, 8 F, age: 68.5±4.24) healthy volunteers participated. The study has the ethics committee approval and all participants signed informed consent. All of the subjects were reported with no clinical evidence of neurologic disease. Geriatric Depression Scale (Ertan, 2000) was applied to old subjects (score: 8.2±3.65). Because of registration issues 1 young and 1 old participant were excluded from segmentation analysis.

2.2 MR Acquisition

Total duration of data collection was about 30 min. High resolution 3D MPRAGE images were obtained via 3.0 Tesla Siemens Magnetom Trio MR Scanner at the UMRAM MR Center in Bilkent University. (TR=2500 ms, TE=3.16 ms, Bandwidth=199 Hz/Pixel, matrix 256*256, Slice Thickness 1 mm,

256 slices, FOV=256*256 (axial), Number of Averages=1).

4 FLASH images were acquired with four different flip angles (3˚, 5˚, 15˚, 30˚) (TR=20 ms, TE=4.15 ms, Bandwidth=199 Hz/Pixel, matrix 256*256, Slice Thickness 3 mm, 44 slices, FOV=256*256 (axial), Number of Averages=1).

We used standard MPRAGE and FLASH protocols because they are widely available and allow for estimation of T_1 tissue characteristics which we wanted to investigate.

2.3 T_1 Mapping

The MR signal consists of several components. T1 is the longitudinally decaying component with respect to time in the MR signal. By estimating T_1 characteristics and using them instead of intensity values, contrast between brain tissues can be increased. Variable flip angle (VFA) method is used for the purpose of T_1 mapping of whole brain such that at least 3 images should be gathered with three different contrasts. VFA approach was shown to be a practical alternative to conventional methods, providing better precision and speed.

One of the most suitable sequences for VFA method is FLASH (Fischl, 2004). The intensity value I(x,y,z) observed in the (x,y,z) voxel of a FLASH image can be written in terms of tissue characteristics and scanning parameters TR (repetition time), TE (echo time), α (flip angle) as follows:

$$I(x,y,z) = \frac{M_0(x,y,z)\, e^{-TE/T_2^*} \sin(\alpha)(1-e^{-TR/T_1}))}{(1-\cos(\alpha)\, e^{-TR/T_1})} \qquad (1)$$

The aim is to use the multiple FLASH images for estimating T_1 tissue value voxelwise.

Then segmentation or other automatic image processing procedures can be based on T_1 maps instead of intensity value of the voxel. For really small α values (e.g. α=3˚) cos(α) approaches to 1 and the equation (1) can be reduced as follows (Buxton, 2002):

$$I(x,y,z) = M_0(x,y,z)\, e^{-TE/T_2^*} \sin(\alpha) \qquad (2)$$

This way, the intensity value of α=3˚ image is described as the constant c=M_0(x,y,z) e^{-TE/T_2^*}sin(3). Therefore, the first part of the eq. (1) can be determined just by using from the image with FA 3˚.

The remaining part of the equation is as follows:

$$I_\alpha(x,y,z) = \frac{c(\sin(\alpha)/\sin(3))\,(1-e^{-TR/T_1}))}{(1-\cos(\alpha)\, e^{-TR/T_1})} \qquad (3)$$

In this equation, $I_\alpha(x,y,z)$ is the intensity value with 5˚, 15˚ and 30˚ flip angles, respectively and c is obtained from the image with α =3˚. Since TR is a known parameter coming from scanning protocol, we need to find T$_1$ value which is the only unknown parameter by using 3 equations derived from 3 images which is an over-determined case. We can compute the T$_1$ value with least squares estimation method as follows:

According to literature T$_1$ ranges between 0-4000 ms. The intensity value for α=5˚, 15˚ and 30˚ is computed based on eq. (3) for all of the candidate T$_1$ values. Then, computed theoretical I$_\alpha$ for each T$_1$ and measured real I$_\alpha$ in image is subtracted and squared. The T$_1$ value of the I$_\alpha$ which has the smallest error is assigned as the T$_1$ value of that particular voxel (i.e. LSE fit).

2.4 Overview of Data Processing

The image processing and signal evaluation pipeline is depicted in Figure 1.

2.4.1 Pre-processing

First step of pre-processing is normalizing the intensities of images acquired from different MRI sequences.

Then, semi-automated removal of skull and non-brain parts is performed using FSL's brain extraction tool (BET) with proper options which attempt to reduce image bias, and residual neck voxels (Smith, 2002). This process provides a basis for a better segmentation.

After brain extraction, FAST (FMRIB's Automated Segmentation Tool) was used for construction of the estimated restored input image after correction for bias field as well as segmenting the MPRAGE into GM, WM, and CSF classes (Zhang et al., 2001). FSL has a superior segmentation procedure for segmentation of sub-cortical area, but this was not utilized in our study. FAST has the ability to give an output per each tissue class and these are binary images which will be used as a mask later. However, since T$_1$ maps were synthetically produced, package programs like FSL failed to produce segmented volumes. Because of this problem, T$_1$ maps were segmented by manual thresholding. T$_1$ values reported in literature as follows: $T_{1WM} \le 1074$ ms, $1074 \le T_{1GM} \le 1359$ ms and $1400 \le T_{1CSF} \le 4000$ ms. All of the images were registered to the standard stereotaxic space (Talairach and Tournoux, 1988). The brain volumes were warped (using 12-parameter affine transform) to TT_N27+tlrc template volume.

Alignment of T$_1$ maps and MPRAGE images was accomplished by using AFNI.

In order to obtain T$_1$ values of a specific brain tissue type voxel-by-voxel arithmetic on 3D datasets was calculated by using AFNI's calculator program. In our case, T$_1$ estimated image and GM mask were multiplied. Hence the resulting image contains T$_1$ values belonging to only GM and everything else is zero. The same procedure was repeated for all of the three tissue types and average T$_1$ values of each one were determined.
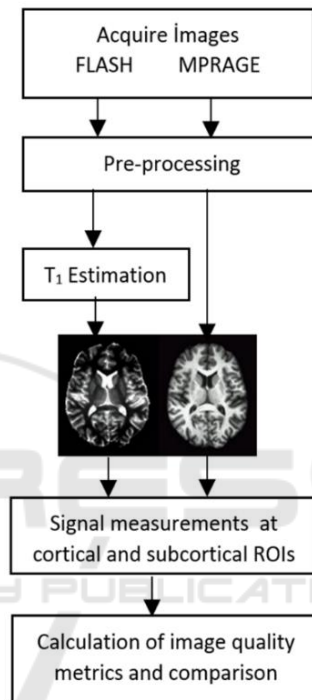

Figure 1: Image processing and signal evaluation pipeline.

2.4.2 Signal Measurements within ROIs

Two subcortical and three cortical GM landmarks were defined to demonstrate age dependent alterations in tissue characteristics. Cortical ROIs were as follows: Rostral Medial Frontal Gyrus (RMFG), crossing point of Superior Frontal Sulcus and Pre-central Sulcus (SFPC), Posterior Central Gyrus (PCG). Caudate and Putamen were chosen as subcortical landmarks (Fig. 2). Also four adjacent WM regions that are neighboring to defined GM ROIs were specified to be able to study Gray-to-White signal Ratios –GWR (adjacent regions were chosen on purpose because they bear similar artefacts based on flip angle inhomogeneity).

Caudate and Putamen are landmarks much studied in T$_1$ mapping literature. RMFG is an important landmark which has a strong reduction in

WM but not GM in aging (Salat et al., 2009). PCG is a prominent structure in the parietal lobe at the crossing of post-central and central sulci and the primary sensory area of the cerebral cortex. According to a study by Salat et al., (2009) the superior frontal gyrus showed a remarkable signal change with age.
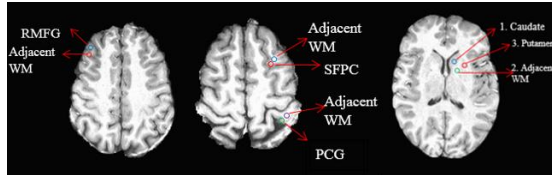

Figure 2: Cortical and subcortical landmarks.

There are several different metrics from which image quality can be inferred. In a high quality image, the measured signal must be higher than noise, the contrast between different tissue types should be high and gray to white ratio should not be close to 1 so that GM and WM structures are identifiable from each other. During aging, these features should be preserved, so that automated morphological analyses derived from adult brains are applicable. Some important metrics in this regard are defined as follows.

Signal-to-Noise Ratio (SNR): SNR is calculated by dividing the mean of tissue intensity to the standard deviation of background noise (Lu, 2005) (background noise is measured from Corpus Callosum since its intensity distribution is homogeneous).

$$SNR = S_{MEAN}/SD_{noise} \qquad (4)$$

Contrast-to-Noise Ratio (CNR): The CNR is a combination of both contrast and SNR. The difference between SNR values of two tissue types gives information about CNR (Lu, 2005).

$$CNR = SNR_{WM} - SNR_{GM} \qquad (5)$$

Gray-to-White Ratio (GWR): GWR is the proportion of the GM signal intensity to that of WM. The power of this metric comes from the dependence on only mean of the tissue signals, not noise.

$$GWR = S_{GM}/S_{WM} \qquad (6)$$

In the worst case, the intensities of two different tissues would be equal and the GWR approximates to 1. The intensity characteristics of the MPRAGE and T_1 maps are reversed (i.e. $T_{1CSF} \geq T_{1GM} \geq T_{1WM}$, while $I_{WM} \geq I_{GM} \geq I_{CSF}$ in MPRAGE). This situation requires

a normalization for measuring the absolute distance of GWR from 1. The absolute distance from 1 gives the information about the distinguishability of the tissues and will be mentioned as 'scaled GWR' in the rest of this article.

2.5 Sub-cortical Segmentation, Sensitivity and Specificity

For the comparison of labels and evaluation of segmentation performance Desai atlas (Destrieux et al., 2010) is chosen. A dilated mask based on this atlas is created for the subcortical structures including Caudate, Putamen, Thalamus and Globus Pallidus. The segmented GM volumes of MPRAGE and T_1 maps were multiplied by this mask and sensitivity and specificity were calculated to evaluate if sub-cortical GM is accurately measured.

True Positive Rate (Sensitivity): Sensitivity relates to the ability of the segmented images to correctly detect GM that is labelled as GM in the atlas. In other words, sensitivity (TPR) of the segmentation is the proportion of the voxels labelled as GM that is labelled as GM in atlas, expressed as follows:

$$Sensitivity = \frac{number\ of\ TP}{number\ of\ TP + number\ of\ FN} \qquad (7)$$

True Negative Rate (Specificity): Specificity (TNR) relates to the segmentation's ability to correctly reject voxels that are not labelled as GM in atlas. Mathematical formulation is as follows:

$$Specificity = \frac{number\ of\ TN}{number\ of\ TN + number\ of\ FP} \qquad (8)$$

3 RESULTS

3.1 Signal Characteristics

For signal measurements, average values of the ROIs are compared between subject groups via repeated measures ANOVA. The outcomes are presented graphically in Figure 3.

3.1.1 GWR Cortical Measurements

There is a significant main effect of image type on GWR (F (1, 15) = 156.073, p<.001, η_p^2=.912). T_1 maps have a higher scaled GWR corresponding to a better contrast (M=2.323, SE=.130) than MPRAGE images (M=.737, SE= .130). However, GWR did not

differ significantly between young and old subjects. The interaction between age and image type also did not differ significantly.

3.1.2 GWR Subcortical Measurements

There is a significant main effect of image type on GWR (F (1, 15) = 426.150, p<.001, η_p^2=.966). T_1 maps have a higher scaled GWR corresponding to a better contrast (M=1.392, SE=.005) than MPRAGE images (M=.753, SE= .032). However, GWR did not differ significantly between young and old subjects. The interaction between age and image type also did not differ significantly.

3.1.3 SNR Cortical Measurements

There is a marginally significant main effect of image type on SNR (F (1, 15) = 4.281, p=.056, η_p^2=.222). T_1 maps have a higher SNR (M=28.298, SE=4.264) than MPRAGE images (M=18.517, SE=1.66). Additionally, SNR differs significantly between young (M=28.608, SE=3.218) and old subjects (M=18.207, SE=3.034) (F (1, 15) = 5.531, p<.05, η_p^2=.269). The interaction between age and image type did not differ significantly.

3.1.4 SNR Subcortical Measurements

There is no significant main effect of image type on SNR. However, SNR differs significantly between young (M=34.362, SE=4.130) and old subjects (M=18.870, SE=3.894) (F (1, 15) = 7.448, p<.05, η_p^2=.332). The interaction between age and image type did not differ significantly.

3.1.5 CNR Cortical Measurements

There is a significant main effect of image type on CNR (F (1, 15) = 11.102, p<.01, η_p^2 =.425). T_1 maps have a higher CNR (M=16.043, SE=2.618) than MPRAGE images (M=6.900, SE=.439). Additionally, CNR differs significantly between young (M=15.637, SE=1.864) and old subjects (M=7.306, SE=1.757) (F (1, 15) = 10.578, p<.01, η_p^2 =.414). The interaction between age and image type did not differ significantly.

3.1.6 CNR Subcortical Measurements

There is no significant main effect of image type on CNR. However, CNR differs significantly between young (M=10.384, SE=1.118) and old subjects (M=5.449, SE=1.055) (F (1, 15) = 10.310, p<.01,

η_p^2=.407). The interaction between age and image type did not differ significantly.

3.2 Segmentation

In Figure 4, TPR and TNR are overlaid to T_1 maps and MPRAGE images of young and old exemplar participants. While TNR looks like similar in both segmented images, TPR is better in T_1 maps. Although segmentation of T_1 maps is conducted through a crude method (i.e. thresholding), segmentation of MPRAGE images failed to detect some important subcortical structures like putamen and thalamus.

3.2.1 True Positive Rate (Sensitivity)

Image type has a significant main effect on the True Positive Rate (TPR) (F(1,15)=111.892, p<.001, η_p^2=.882). The sensitivity of T_1 maps (M=.546, SE=.012) is higher than MPRAGE (M=.344, SE=.012). There is no interaction between image type and age. There is no significant difference between young and old subjects' sensitivity (Figure 5 a).

3.2.2 True Negative Rate (Specificity)

Image type does not significantly affect the True Negative Rate (TNR). There is no interaction between image type and age. There is no significant difference between young and old subjects' specificity (Figure 5 b).

3.3 Comparison of T_1 across Age Groups

To investigate T_1 spin-lattice relaxation time alterations through aging, all of the five GM landmarks (Table 1) and four adjacent WM (Table 2) were evaluated in both old and young subjects. T_1 values between two populations were tested with independent samples t-test and the outcomes are summarized in the following tables. T_1 prolongation with aging was an expected result, hence all of the GM structures except for posterior central gyrus, adjacent WM between caudate and putamen and adjacent WM to RMGF showed prolonged values with increasing age (p≤.05). We found that average T_1 value of young subjects is 605±129 ms for WM and 1147.4±194 ms for GM. Estimated T_1 value for olds is and 733±141 ms 1399.4±135 ms for GM.

Table 1: Statistics of GM ROIs in perspective of Spin-Lattice Relaxation Time (T_1) (ms).

ROI	Age	Mean± Std. Err	t	p
Caudate	Young	1213±32	2.226	.040
	Old	1331±41		
Putamen	Young	1220±24	2.423	.027
	Old	1339±41		
RMFG	Young	895±111	4.048	.001
	Old	1593±129		
PCG	Young	1438±124	1.413	.176
	Old	1221±95		
SFPC	Young	971±86	3.807	.001
	Old	1513±110		

(RMFG: Rostral middle frontal gyrus, PCG: Posterior-central gyrus, SFPC: crossing point of Superior Frontal Sulcus and Pre-central Sulcus).

Table 2: Statistics of WM ROIs in perspective of Spin-Lattice Relaxation Time (T_1) (ms).

ROI	Age	Mean± Std. Err	t	p
CP adj. WM	Young	848±21	3.500	.003
	Old	979±30		
RMFG adj. WM	Young	579±70	2.271	.036
	Old	758±40		
PCG adj. WM	Young	517±51	-.565	.579
	Old	565±65		
SFPC adj. WM	Young	480±66	1.932	.070
	Old	633±47		

(CP adj. WM: Adjacent WM between caudate and putamen, RMFG adj. WM: Adjacent WM to RMGF, PCG adj. WM: Adjacent WM to PCG, SFPC adj. WM: Adjacent WM to SFPC).

4 DISCUSSION AND CONCLUSION

Standard MRI sequences are composed of multiple MR tissue properties such as T_1 and T_2 relaxation times prohibiting direct mapping from pixel intensity to tissue classification. This study demonstrated that usage of intrinsic tissue parameters such as T_1 spin-lattice relaxation time instead of tissue signal intensities produces a more valid metric to detect age-related microstructural changes in healthy ageing providing a better scaffold for tissue segmentation. Unfortunately, small sample size is an important limitation of our study. The following interpretations and conclusions should be considered bearing this limitation in mind.

In our study, estimated T_1 values are consistent with literature (Lu et al., 2005; Marques et al., 2010; Deoni et al., 2005; Okubo et al., 2017). A future study

can be conducted to determine the accuracy of FLASH images in estimating T_1 maps in comparison to MP2RAGE images. Interestingly, our findings with respect to prolongation of T_1 in aging agree with only some studies (Cho et al., 1997), while contradict with others (Saito et al., 2009; Gracien et al., 2017). A recent study demonstrated that age-related changes in T_1 relaxation time vary by location in deep GM (Okubo et al., 2017). When the relationship between T_1 prolongation, axonal loss (van Waesberghe et al., 1999) and demyelination of WM is considered, interpretation of interpretation of the discrepancies of T1 values in the aging brain becomes a hard problem. Conducting a longitudinal study instead of cross-sectional might provide valuable information since T_1 mapping is sensitive to age-related microstructural changes.

Additionally, the characterization of signal changes in healthy aging provides important information that is complementary to morphometric studies of regional brain volumes (Davatzikos and Resnick, 2002). In segmentation analysis, T_1 maps have definitely better sensitivity (54.6%) than MPRAGE images (34.4%) although specificity did not differ significantly between two images. As future work, segmentation of T_1 maps can be evaluated with modern segmentation methods so that the utilities provided by T_1 mapping in the aging brain becomes obvious.

In terms of signal calculations GWR computation has several advantages over other signal computations: For both cortical and subcortical areas, T_1 maps are inarguably better than MPRAGE. Furthermore, in T_1 maps, signal characteristics did not degrade in the aged population. For other measures such as SNR and CNR, T_1 maps have superiority compared to MPRAGE on cortical level. Unfortunately, both SNR and CNR revealed degradation through.

Overall, for several signal characteristics, T_1 maps have better quality because unlike conventional MR protocols, the signal quality does not degrade over aging.
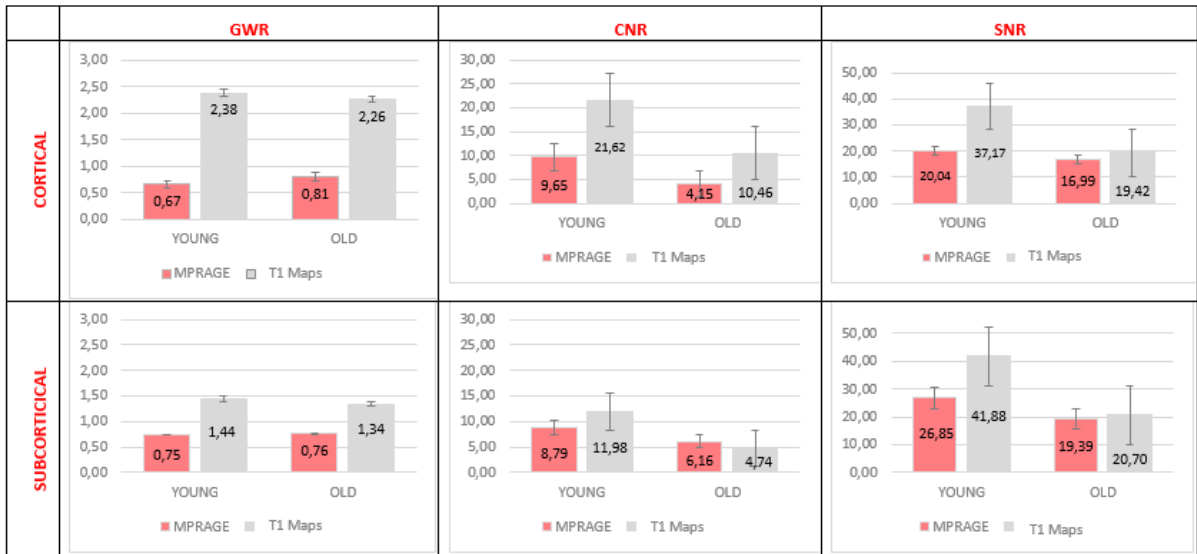
Figure 3: Comparison of GWR, CNR and SNR of young and old population as well as image type (MPRAGE vs T_1 maps).
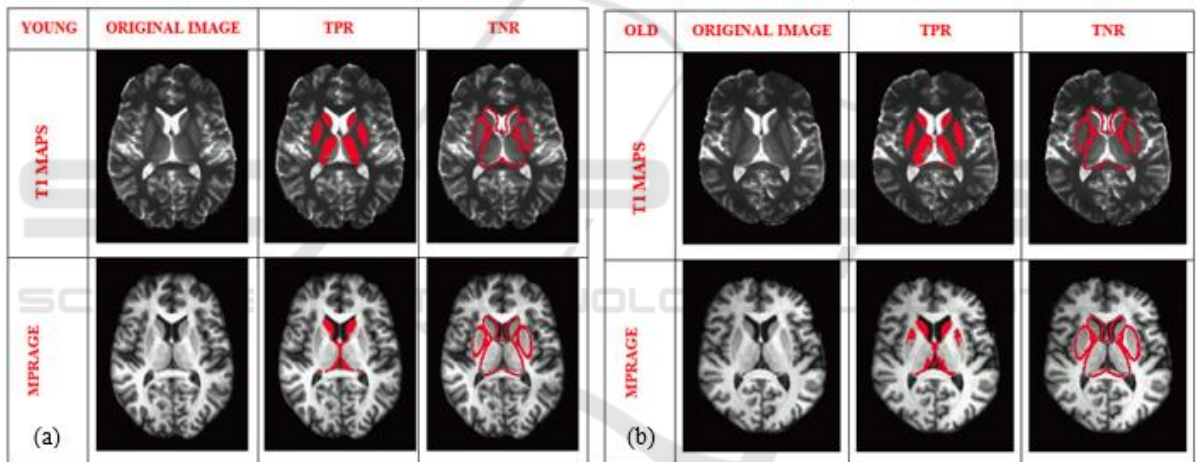

Figure 4: Comparison of gray matter segmentation performance of MPRAGE and T_1 maps, sensitivity and specificity measures of a young (a) and old (b) subject.
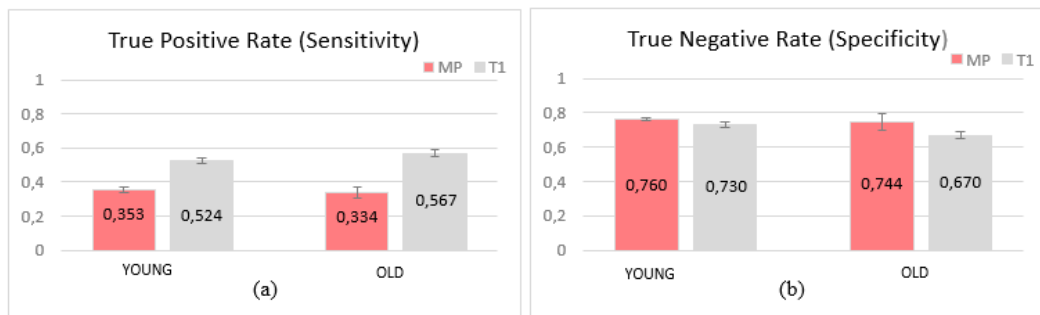

Figure 5: Sensitivity (a) and Specificity (b) values of both populations and image types (MP: MPRAGE, T1: T_1 map.

REFERENCES

Buxton, R. B. (2009). Introduction to functional magnetic resonance imaging: principles and techniques. Cambridge university press.

Cho, S., Jones, D., Reddick, W. E., Ogg, R. J., & Steen, R. G. (1997). Establishing norms for age-related changes in proton T1 of human brain tissue in vivo. Magnetic resonance imaging, 15(10), 1133-1143.

Courchesne, E., Chisum, H. J., Townsend, J., Cowles, A., Covington, J., Egaas, B.& Press, G. A. (2000). Normal brain development and aging: quantitative analysis at in vivo MR imaging in healthy volunteers. Radiology, 216(3), 672-682.

Davatzikos, C., & Resnick, S. M. (2002). Degenerative age changes in white matter connectivity visualized in vivo using magnetic resonance imaging. Cerebral cortex, 12(7), 767-771.

Deoni, S. C., Peters, T. M., & Rutt, B. K. (2005). High-resolution T1 and T2 mapping of the brain in a clinically acceptable time with DESPOT1 and DESPOT2. Magnetic resonance in medicine, 53(1), 237-241.

Desmond, K. L., Al-Ebraheem, A., Janik, R., Oakden, W., Kwiecien, J. M., Dabrowski, W. & Bock, N. A. (2016). Differences in iron and manganese concentration may confound the measurement of myelin from R1 and R2 relaxation rates in studies of dysmyelination. NMR in Biomedicine, 29(7), 985-998.

Destrieux, C., Fischl, B., Dale, A., & Halgren, E. (2010). Automatic parcellation of human cortical gyri and sulci using standard anatomical nomenclature. Neuroimage, 53(1), 1-15.

Ertan, T., & Eker, E. (2000). Reliability, validity, and factor structure of the geriatric depression scale in Turkish elderly: are there different factor structures for different cultures?. International Psychogeriatrics, 12(2), 163-172.

Fischl, B., Salat, D. H., van der Kouwe, A. J., Makris, N., Ségonne, F., Quinn, B. T., & Dale, A. M. (2004). Sequence-independent segmentation of magnetic resonance images. Neuroimage, 23, S69-S84.

Ge, Y., Grossman, R. I., Babb, J. S., Rabin, M. L., Mannon, L. J., & Kolson, D. L. (2002). Age-related total gray matter and white matter changes in normal adult brain. Part I: volumetric MR imaging analysis. American journal of neuroradiology, 23(8), 1327-1333.

Gracien, R. M., Nürnberger, L., Hok, P., Hof, S. M., Reitz, S. C., Rüb, U. & Baudrexel, S. (2017). Evaluation of brain ageing: a quantitative longitudinal MRI study over 7 years. European radiology, 27(4), 1568-1576.

Lu, H., Nagae-Poetscher, L. M., Golay, X., Lin, D., Pomper, M., & van Zijl, P. (2005). Routine clinical brain MRI sequences for use at 3.0 Tesla. Journal of Magnetic Resonance Imaging, 22(1), 13-22.

Marques, J. P., Kober, T., Krueger, G., van der Zwaag, W., Van de Moortele, P. F., & Gruetter, R. (2010). MP2RAGE, a self bias-field corrected sequence for improved segmentation and T 1-mapping at high field. Neuroimage, 49(2), 1271-1281.

Ogg, R. J., & Steen, R. G. (1998). Age-related changes in Brain T1 are correlated with iron concentration. Magnetic resonance in medicine, 40(5), 749-753.

Okubo, G., Okada, T., Yamamoto, A., Fushimi, Y., Okada, T., Murata, K., & Togashi, K. (2017). Relationship between aging and T1 relaxation time in deep gray matter: A voxel-based analysis. Journal of Magnetic Resonance Imaging.

Resnick, S. M., Goldszal, A. F., Davatzikos, C., Golski, S., Kraut, M. A., Metter, E. J., ... & Zonderman, A. B. (2000). One-year age changes in MRI brain volumes in older adults. Cerebral cortex, 10(5), 464-472.

Saito, N., Sakai, O., Ozonoff, A., & Jara, H. (2009). Relaxo-volumetric multispectral quantitative magnetic resonance imaging of the brain over the human lifespan: global and regional aging patterns. Magnetic resonance imaging, 27(7), 895-906.

Salat DH, Buckner RL, Snyder AZ, Greve DN, Desikan RS, Busa E, Morris JC, Dale AM, and Fischl B. (2004). Thinning of the cerebral cortex in aging. Cereb. Cortex

Salat, D. H., Lee, S. Y., Van der Kouwe, A. J., Greve, D. N., Fischl, B., & Rosas, H. D. (2009). Age-associated alterations in cortical gray and white matter signal intensity and gray to white matter contrast. Neuroimage, 48(1), 21-28.

Smith, S. M. (2002). Fast robust automated brain extraction. Human brain mapping, 17(3), 143-155.

Stikov, N., Boudreau, M., Levesque, I. R., Tardif, C. L., Barral, J. K., & Pike, G. B. (2015). On the accuracy of T1 mapping: searching for common ground. Magnetic resonance in medicine, 73(2), 514-522.

Talairach J, Tournoux P (1988). Co-planar stereotaxic atlas of the human brain. Thieme, New York.

Tau, G. Z., & Peterson, B. S. (2010). Normal development of brain circuits. Neuropsychopharmacology, 35(1), 147-168..

Thambisetty, M., Wan, J., Carass, A., An, Y., Prince, J. L., & Resnick, S. M. (2010). Longitudinal changes in cortical thickness associated with normal aging. Neuroimage, 52(4), 1215-1223.

Van Waesberghe, J. H. T. M., Kamphorst, W., De Groot, C. J., Van Walderveen, M. A., Castelijns, J. A., Ravid, R. & Barkhof, F. (1999). Axonal loss in multiple sclerosis lesions: magnetic resonance imaging insights into substrates of disability. Annals of neurology, 46(5), 747-754.

Wansapura, J. P., Holland, S. K., Dunn, R. S., & Ball, W. S. (1999). NMR relaxation times in the human brain at 3.0 tesla. Journal of magnetic resonance imaging, 9(4), 531-538.

Zhang, Y., Brady, M., & Smith, S. (2001). Segmentation of brain MR images through a hidden Markov random field model and the expectation-maximization algorithm. IEEE transactions on medical imaging, 20(1), 45-57.